The Actin-Binding Protein Hisactophilin Binds in Vitro to Partially Charged Membranes and Mediates Actin Coupling to Membranes†

Almuth Behrisch,‡ Christian Dietrich,‡ Angelika A. Noegel,§ Michael Schleicher,|| and Erich Sackmann‡,⊥,*

Physik Department, E22 (Biophysical Laboratory), Technische Universität München, James Franck Strasse, D-85747 Garching, FRG, Max-Planck-Institut für Biochemie, Am Klopferspitz 18a, D-82152 Martinsried, FRG, and Institut für Zellbiologie, Fakultät für Medizin, Ludwig Maximilians Universität München, Schillerstrasse 42, D-80336 München, FRG

Received April 21, 1995; Revised Manuscript Received August 28, 1995⊗

ABSTRACT: The interaction of the actin-binding protein hisactophilin from *Dictyostelium discoideum amoebae* to partially charged lipid membranes composed of mixtures of L-α-dimyristoylphosphatidylcholine (DMPC) with L-α-dimyristoylphosphatidylglycerol (DMPG) and L-α-phosphatidylinositol 4,5-bisphosphate (PIP_2) is studied by film balance experiments, microfluorescence, and lateral diffusion measurements at low ionic strengths (~20 mM). Excess surface concentrations and adhesion energies of the protein are evaluated by the application of Gibbs law of surface excess as a function of charged lipid content. Protein expressed in *E. coli* lacking a myristic acid chain (EC-HIS) and natural protein with a fatty acid (DIC-HIS) isolated from *Dictyostelium* cells are compared. For mixtures of DMPG and DMPC, protein binding leads to an increase in lateral pressure of the monolayer (at constant area) and causes strong lipid immobilization pointing to partial penetration of the protein into the lipid layer. The natural protein causes a much stronger immobilization than does EC-HIS. For a given bulk concentration, the adsorbed protein/lipid molar ratio increases with the molar fraction x_{PG} of charged lipid but saturates at about 50 mol% of DMPG. Natural hisactophilin (DIC-HIS) binding to PIP_2-containing monolayers is purely electrostatic at low bulk concentration c_b, and protein penetration dominates only at c_b >68 nM. Fluorescence experiments demonstrate that the natural protein (DIC-HIS) can mediate the binding of monomeric actin or very small oligomers to membranes, showing that the adsorbed protein remains functional. In contrast, the recombinant hisactophilin (EC-HIS) can mediate only the membrane coupling of larger actin structures.

The mechanism of coupling actin to plasma membranes is still poorly understood although several actin−membrane coupling proteins are known (for references see Isenberg, 1991). The best studied example is talin which, in combination with vinculin, is supposed to mediate the coupling of actin filaments to lipid membranes by binding to integral membrane proteins (Goldmann et al., 1992). Most direct *in vitro* evidence for the important role of talin for the cytoskeleton−membrane interaction comes from findings that talin incorporates into lipid membranes and also binds to actin (Kaufmann et al., 1992). Another actin-binding protein that is supposed to mediate the binding of actin to the membrane is hisactophilin, a 13.5 kDa protein of *Dictyostelium discoideum* (Scheel et al., 1989). A common outstanding feature of hisactophilin is that it binds to actin at a pH <7 and is completely released at pH values >7.5 (Scheel et al., 1989). The NMR structure of hisactophilin shows an intrinsic polarity of the molecule which is composed exclusively of beta strands and loops (Habazettl et al., 1992). The N- and C-termini are harbored in a tightly packed beta-barrel conformation. The loops, however, are loosely organized at the opposite end of the molecule. They are connected to beta hairpins and carry almost all of the histidine residues. This suggests an interaction with the plasma membrane such that the uncharged barrel structure points toward the membrane, whereas the histidine-rich loops face the cytoplasm and organize the binding to filamentous actin in a pH-dependent manner. The interaction with the membrane is greatly enhanced by a myristic acid chain at the N-terminus on top of the beta-barrel structure (Hanakam et al., 1995). Two common properties of talin and hisactophilin are: 1. Only a fraction of the protein is associated with the membrane (about 50% in the case of hisactophilin; see Hanakam et al., 1995; Scheel et al., 1989) while the rest is distributed within the cytoplasm. 2. At moderate ionic strengths these proteins bind directly to lipid bilayers in the presence of charged lipids. In the case of talin it has been shown that such electrostatically bound proteins can mediate the coupling of actin filaments to lipid bilayer vesicles (Kaufmann et al., 1992).

To investigate the mechanism of the interaction of hisactophilin with artificial lipid layers, it was therefore essential to compare its binding to membranes in the presence and absence of myristic acid. This allowed us to compare the contributions of electrostatic forces and the hydrophobic effect (due to the fatty acid penetration into the lipid lamellae) to membrane coupling of the protein. For that purpose we

† This work was supported by the Deutsche Forschungsgemeinschaft (DFG-SFB 266) and the Fonds der chemischen Industrie. The research was further supported by the National Science Foundation under Grant No. PHY 8904035 and by grants from the European Union to A.A.N. and M.S.

* To whom correspondence should be addressed.
‡ Technische Universität München.
§ Max-Planck-Institut für Biochemie.
|| Ludwig Maximilians Universität München.
⊥ On leave, visiting the Institute for Theoretical Physics, University of California, Santa Barbara, CA 93106, U.S.A.

⊗ Abstract published in *Advance ACS Abstracts,* October 15, 1995.

0006-2960/95/0434-15182$09.00/0

studied bacterially expressed hisactophilin (denoted EC-HIS)[1] which does not carry a myristic acid at the N-terminus (Scheel et al., 1989; Habazettl et al., 1992), and a myristoylated hisactophilin (designated as DIC-HIS) from a *Dictyostelium discoideum* transformant (Stöckelhuber et al., unpublished results).

In the present work, we measured the interaction of the two types of hisactophilin with partially charged lipid monolayers composed of DMPC and either DMPG or PIP_2 (cf. list of abbreviations) of various composition. The film balance technique was applied to study the hisactophilin−membrane interaction since it allows us to investigate the influence of the lateral lipid packing density and the lateral pressure on the lipid−protein interaction in a systematic way. Denaturation of the protein can be avoided by keeping the lateral pressure well above the equilibrium spreading pressure of the protein. Protein binding can be evaluated (1) by recording the variation of the lateral pressure at constant area caused by addition of the protein to the subphase, and (2) by microfluorescence observation of fluorescent protein. In the present work we measured the surface excess concentration of both modifications of the protein by application of the Gibbs equation as a function of the charged lipid concentration. From these measurements, the chemical potential difference of the protein in the bulk solution and the protein bound to the membrane was obtained as a quantitative measure of the strength of lipid−protein interaction. The lipid−protein interaction was further characterized by measuring the variation of the lipid lateral diffusion coefficient by photobleaching experiments. A most remarkable result is the strong reduction of the lipid mobility by the protein, showing that the protein binding substantially affects the membrane structure. Although this holds for both the natural and the fatty acid-depleted protein, the decrease in lipid mobility, caused by the two species is different. This finding shows the important role of the fatty acid chain for the protein−membrane coupling and indicates that the binding of the native and the recombinant hisactophilin to the membrane surface is remarkably different. Recently this difference was directly demonstrated by neutron surface reflectivity measurements (Naumann, to be published) as will be reported in a forthcoming paper.

EXPERIMENTAL PROCEDURES

Materials. EC-HIS was expressed in *E. coli* essentially as described (Scheel et al., 1989). Because in *D. discoideum* two very closely related hisactophilin isoforms 1 and 2 are present (Hanakam et al., 1995), we used for protein purification a transformant that was deficient in hisactophilin 1 and overexpressed hisactophilin 2. This was achieved by a gene replacement in the hisactophilin 1 gene and a tandem integration of the hisactophilin 2 gene with its own promoter (Stöckelhuber et al., unpublished results). The presence of myristic acid was confirmed by mass spectrometry. Purification of both EC-HIS and DIC-HIS was done as described by Scheel et al. (1989) with an additional purification step over an ion-exchange FPLC column (Stöckelhuber et al., unpublished results). Briefly, the hisactophilin-containing fractions were loaded onto an anion-exchange column (MonoQ, Pharmacia, Freiburg) at first at a pH of 6. Under these conditions the molecule is positively charged and remains in the flowthrough. After raising of the pH to 7.8, reequilibration of the column, and binding of the now negatively charged hisactophilin to the same column, all major contaminants could be removed by eluting the protein with a salt gradient (0−500 mM NaCl).

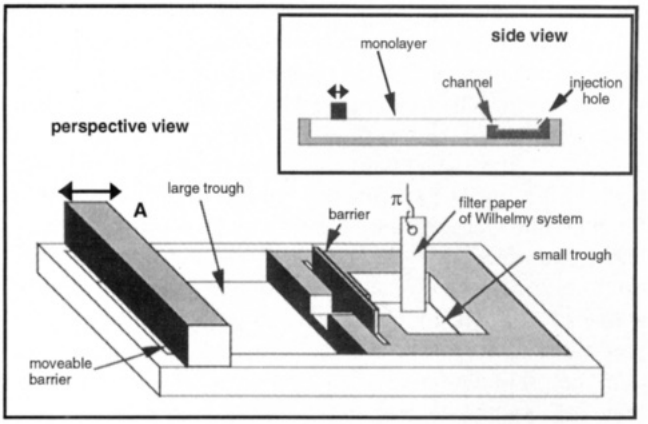

FIGURE 1: Schematic view of the film balance consisting of a large trough and a compartment (small trough) for protein-binding studies. The monolayers of the main trough and the measuring compartment are connected by a thin channel of 5 × 4 mm^2 cross section and 15 mm length. The lateral pressure is measured within the compartment by a Wilhelmy plate. The total area of the small trough is kept constant by closing the channel with a small barrier.

G-actin was prepared according to Pardee and Spudich (Pardee & Spudich, 1982) with an additional gel filtration step using a Sepharcryl S-300 column. Actin was labeled with NBD (denoted as NBD-actin) exactly as described by Detmers et al. (1981).

DMPG and DMPC, supplied from Avanti Polar Lipids (Birmingham, Alabama, U.S.A.), were dissolved in chloroform/methanol solution 9/1 (v/v). The stock solution of PIP_2, purchased from Sigma Chemie (Deisenhofen, Germany), was prepared with a chloroform/methanol solution 3/1 (v/v). To allow observation of the lipid films with the fluorescence microscope, small amounts of the fluorescent lipid TR-PE from Molecular Probes (Eugene, Oregon, USA) were added to the solutions (0.1 mol%). The various lipid mixtures were spread onto an aqueous solution (subphase), containing 10 mM Hepes buffer, 10 mM NaCl, 0.25 mM EDTA, and 0.25 mM EGTA. Different pH values were adjusted by addition of NaOH. All experiments were performed at 20 °C.

Methods. Monolayer experiments were performed with two types of film balances. For the stepwise injection experiments, we used a large film balance with a dimension of 9 × 45 × 0.5 cm^3. A small trough (surface area: 7.6 cm^2; volume: 3.6 cm^3) was inserted into the large trough in such a way that the two compartments were connected by a thin channel (cf. Figure 1). The pressure π of a spread monolayer could be varied by a moveable barrier in the outer trough. After adjustment of the desired pressure, the two compart-

[1] Abbreviations: DIC-HIS, hisactophilin from *Dictyostelium discoideum*; EC-HIS, hisactophilin from *Escherichia coli*; DMPC, L-α-dimyristoylphosphatidylcholine; DMPG, L-α-dimyristoylphosphatidylglycerol; PIP_2, L-α-phosphatidylinositol 4,5-bisphosphate; NBD-Cl, 7-chloro-4-nitrobenz-2-oxa-1,3-diazole; TR-PE, Texas Red-labeled L-α-dipalmitoylphosphatidylethanolamine; EDTA, ethylenediaminetetraacetic acid; EGTA, ethylene glycol-*O*,*O*′-bis(2-aminoethyl)-*N*,*N*,*N*′,*N*′-tetraacetic acid; Hepes, 4-(2-hydroxyethyl)-piperazine-1-ethanesulfonic acid. *Symbols*: π, lateral pressure in mN/m; Γ, surface excess concentration; c_b, protein concentration in bulk in mol/L; n_s, n_b, protein area concentrations at the interface and in the bulk, respectively, in molecules/nm^2; x_{PG}, molar fraction of DMPG; D, lateral diffusion coefficient of lipids.

ments were separated by a barrier in the channel. Protein was then added to the subphase of the small trough through an injection hole (cf. insert of Figure 1). The Wilhelmy system was installed within the little trough to measure the time evolution of the pressure. A filter paper was used as a Wilhelmy plate. The temperature was regulated by a water bath (±0.2 °C). Experiments with fluorescence-labeled hisactophilin were performed with a microfluorescence film balance, developed by Heyn et al. (1990). The unit consists essentially of a fluorescence microscope which is placed above a Langmuir trough. The microscope is mounted on a motorized $x-y$ translation stage, which allows the observation of most of the fluid surface. Moreover, the fluorescence light can be analyzed by a spectrometer. The base of the large trough is brass-plated, and Peltier elements are fixed to the lower surface of the plate for temperature regulation (±0.2 °C).

The lateral lipid mobility was studied by a simplified photobleaching technique which is described in Appendix A. The same device was used for the analysis of the distribution of fluorescent probes in the normal direction; this allows us to distinguish between molecules in the subphase and at the surface. A more elaborate description of the method is also given in Appendix B.

RESULTS

Analysis of Hisactophilin−Membrane Interaction by Gibbs Equation. In the first series of experiments, we attempted to evaluate the hisactophilin−membrane interaction in terms of the well-known Gibbs equation of adsorption. For this purpose, the variation of the lateral pressure π, induced by the hisactophilin adsorption, was measured at constant area as a function of (1) the lipid composition of the monolayer, and (2) the lateral pressure. For this purpose the lateral pressure was continuously recorded at constant area while aliquots of hisactophilin solution were subsequently injected into the subphase of the measuring compartment separated from the main trough (cf. Figure 1).

After each injection step, the change in pressure was observed for several hours in order to allow equilibration of the protein in the bulk phase by diffusion. New protein was added when the pressure appeared to be saturated. The pressure change was recorded by a Wilhelmy plate within the measuring compartment at constant area. Smaller protein concentrations were added at the beginning of the experiments than toward the end.

Three typical titration experiments are shown in Figure 2a for a lipid mixture containing 30% charged lipid (DMPG) for different initial lateral pressures π_0 (π_0 = 14.7 mN/m, π_0 = 20.6 mN/m, and π_0 = 24.7 mN/m). The amount of protein added per injection was 0.7 μg for the first three steps, 1.05 μg for the fourth step, and 3.15 μg for the fifth and sixth injection step. The subphase volume was 3.6 cm^3, and the above amounts thus correspond to bulk concentrations of 15 nM, 30 nM, 45 nM, 68 nM, 135 nM, and 203 nM. The equilibration time was chosen to be longer after the third and the fifth injection step. The protocol of Figure 2 pertains to all titration experiments unless otherwise noted. Special care was taken to keep the surface pressure of the monolayer above the spreading pressure of the protein (about 10 mN/m for EC-HIS and close to 0 mN/m for DIS-HIS) and to avoid leakage of the measuring trough. A closer

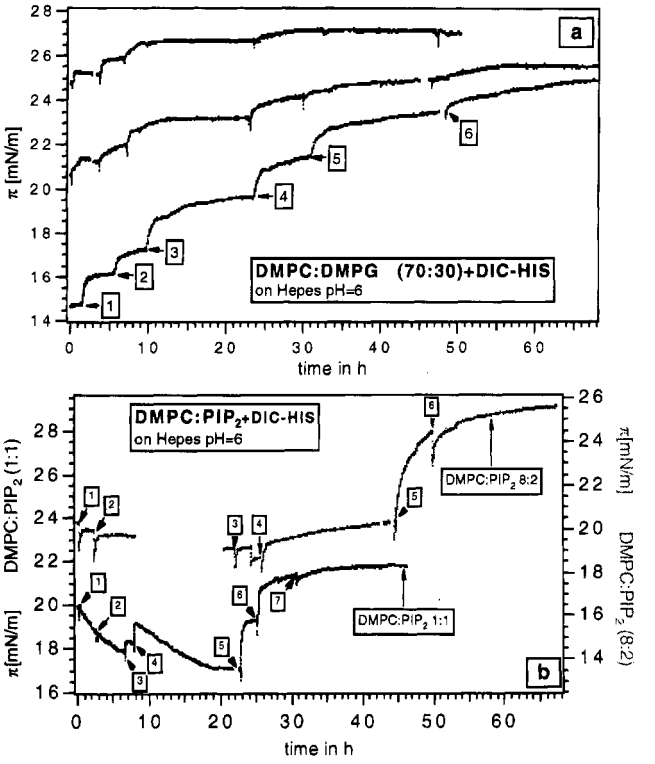

FIGURE 2: (a) Increase of lateral pressure of mixed DMPC/DMPG monolayer containing 30 mol% DMPG caused by stepwise addition of small aliquots of hisactophilin from *Dictyostelium* (DIC-HIS) added at times indicated by arrows. The amount of protein added was 0.7 μg for steps 1−3, 1 μg for step 4, and 3 μg for steps 5 and 6. The buffer (3.6 mL) was Hepes at pH 6. Note that the incremental pressure increase is larger for lower initial pressures and that saturation is reached at a higher bulk protein concentration. (b) Titration curves for a monolayer composed of 80 mol% DMPC and 20 mol% PIP_2 and a monolayer containing 50 mol% DMPC and 50 mol% PIP_2, respectively. The amount of protein added at steps 1−5 is the same as in Figure 2a, but is higher for step 6 (6 μg). Additionally 3 μg DIC-HIS were injected in a 7th step. Note the different scales for the 8:2 mixture (right side) and the 1:1 mixture (left side). The stepwise increased π at steps 3 and 4 for the lower curve is due to the sudden increase of the water level by the injection.

inspection of Figure 2a shows (1) that the pressure increase saturates at high bulk protein concentration, and (2) that the saturation concentration increases with decreasing initial pressure, π_0.

Figure 2b presents titration curves for a mixture of 80 mol% DMPC and 20 mol% PIP_2 and an equimolar mixture of the two lipids, respectively. A remarkable difference compared to the behavior of the DMPC/DMPG mixtures is the initial decrease of the lateral pressure for protein concentration c_b <70 nM (first four injection steps) as compared to the pressure increases at higher protein concentrations. We argue below that this can be rationalized in terms of a purely electrostatic effect at low bulk protein concentrations and a crossover to protein penetration at high c_b values. Figure 2 shows that the change of the pressure saturates more readily for high initial values of π_0 than for low values of π_0.

For a quantitative evaluation of the interaction of hisactophilin with the membranes, the so-called surface excess concentration, Γ, was determined by application of the Gibbs equation. The surface excess Γ (measured in units of molecules per unit area) is the difference between the protein concentration in the adsorbed layer at the surface and within

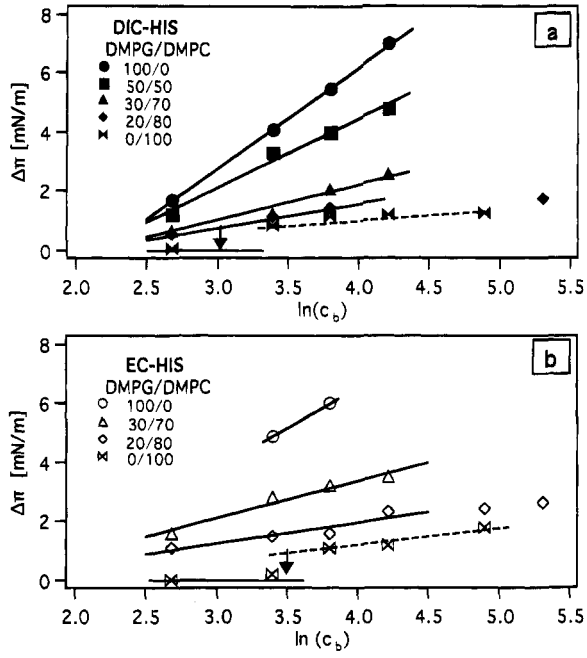

FIGURE 3: Plot of the lateral pressure difference $\Delta\pi = \pi - \pi_0$ (at constant area) as a function of the bulk concentration ln c_b. For all experiments the initial pressure π_0 was about 25 mN/m. (a) Native hisactophilin (DIC-HIS) for DMPG molar fractions x_{PG} = 1.0 (●), 0.5 (■), 0.3 (▲), 0.2 (◆) and for 0 (solid bowties). (b) Hisactophilin expressed in *E. coli* (EC-HIS) for DMPG molar fractions x_{PG} = 1.0 (○), 0.3 (△), 0.2 (◇) and 0 (open bowties). For all experiments the bulk phase consisted of Hepes buffer at pH 6, and the temperature (T) was 20 °C. The straight lines characterize the slopes of the $d(\Delta\pi)/d(\ln c_b)$, which were used to determine Γ.

a thin layer in the bulk solution exhibiting the same thickness as the surface layer.

The Gibbs equation

$$\Gamma = -\frac{1}{k_B T}\cdot\frac{d\gamma}{d\ln c} = -\frac{c_b}{k_B T}\cdot\frac{d\gamma}{dc_b} \qquad (1)$$

relates the surface excess Γ to the change in surface tension of the interface with the variation of the bulk solute concentration c_b. In the film balance experiment, one measures the difference $\pi = \gamma_{H_2O} - \gamma$ between the surface tension of the monolayer-covered (γ) and the free water surface (γ_{H_2O}), respectively. Since the protein is added only to the compartment covered by a monolayer in which the pressure change $\Delta\pi$ is measured by a Wilhelmy film balance, one can assume $\Delta\gamma = -\Delta\pi$. Figure 3a shows plots of $\Delta\pi$ versus ln c_b for natural protein (DIC-HIS) and Figure 3b for protein expressed in *E. coli* (EC-HIS). The excess concentration Γ can be approximately determined from the slopes of the straight-line regime ($\Delta\pi$ vs ln c_b) by application of equation (1). The reciprocal values of Γ obtained by this procedure are plotted in Figure 4 as a function of the molar fraction. Below we determine from these data the chemical potential difference of the protein between the bulk and the surface.

The most pertinent results of Figures 3 and 4 are: 1. For DMPG molar fraction x_{PG} <0.5, the excess concentration increases linearly with the molar fraction of charged lipid but saturates at higher molar fractions. 2. A remarkable excess is found for pure DMPC only above a threshold concentration of ln $c_b \approx 3.0$ for DIC-HIS and ln $c_b > 3.5$ for EC-HIS (indicated in Figure 2 with arrows). The slopes

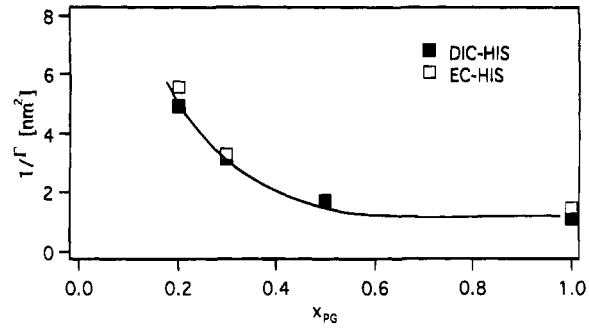

FIGURE 4: Plot of reciprocal excess 1/Γ of hisactophilin as a function of DMPG molar fractions obtained from the slopes of the $\Delta\pi$-versus-ln c_b plots of Figure 3. The drawn curve is included to guide the eye.

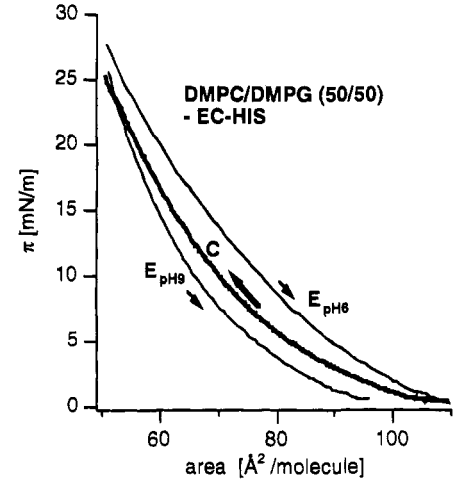

FIGURE 5: Effect of EC-HIS on π-versus-A isotherm of DMPC/DMPG 1:1 mixture observed during expansion. The curve C (thick line) for the pure lipid mixture was recorded during the first compression on a buffer kept at pH 6 which contained no protein. The curves E_{pHx} were obtained during expansion of the film after addition of the protein to the subphase at 25 mN/m and an optional change of the pH value. The different pH values are indicated at the curves. The protocols of the experiments are described in the text.

of the variation of $\Delta\pi$ with c_b (and therefore Γ) below this concentration are too small to be measured.

pH Dependence of Hisactophilin−Membrane Association. The main driving force for the hisactophilin−membrane coupling is the electrostatic interaction between the histidine-rich protein and the partially charged membrane. This follows indirectly by our observations of (1) the strong increase of the surface excess with charged lipid content and (2) the very weak binding of hisactophilin to DMPC monolayers. A more direct proof is the pH dependence of protein adsorption shown in Figure 5 for the case of EC-HIS. A monolayer composed of a 1:1 DMPC/DMPG mixture on a subphase at pH 6 was first compressed to about 25 mN/m (Figure 5, curve C). Then the protein was added at the same pH 6, which caused an increase in pressure as described above. After equilibration for about 1 h, the film was expanded. The isotherm observed (curve E_{pH6} in Figure 5) remains shifted to larger areas in comparison to the compression without the protein in the subphase (cf. transition from curve C to curve E_{pH6}). The reversibility of this effect was demonstrated in a separate experiment. Therefore, the protein was again injected into the subphase of a compressed 1:1 DMPC/DMPG monolayer (25 mN/m) at pH

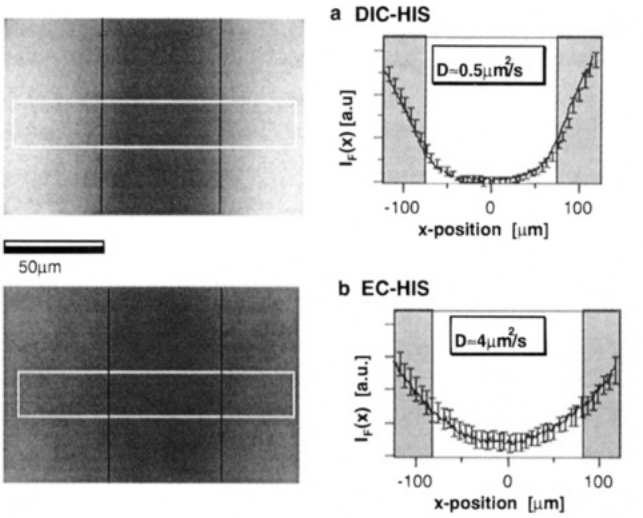

FIGURE 6: Illustration of lateral diffusion measurement by continuous bleaching technique. In a lipid monofilm dissolved fluorescent-labeled lipid (TR-PE, cf. list of abbreviations) is bleached along a stripe of about 160 μm width indicated by the two dark vertical straight lines. For that purpose, the circular aperture is replaced by a slit. The bleaching process is performed until the fluorescence intensity in the bleached region does no longer change with time. The slit is removed, and the fluorescence intensity is measured by means of a camera and recorded on video tape. The intensity distribution $I_F(x)$ in a direction perpendicular to the stripe is analysed in the restricted area indicated by the bright frame in the left image by an image processing unit. Fitting of $I_F(x)$ by the diffusion equation (as described in Appendix A) yields approximate values of the diffusion coefficient D. Addition of (a) DIC-HIS and (b) EC-HIS in the subphase (pH 6, protein $c_b = 93$ nM protein) of a DMPC/DMPG 1:1 monolayer (25 mN/m) leads to different bleach profiles corresponding to different diffusion coefficients.

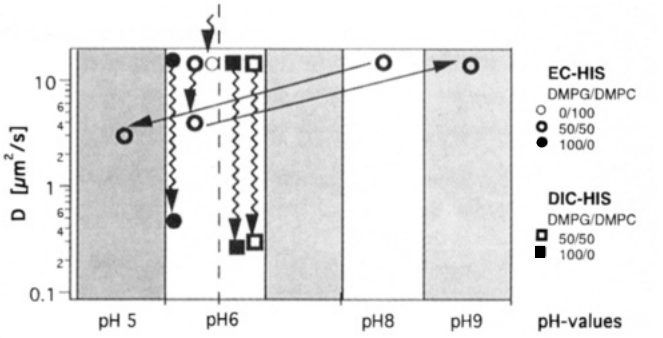

FIGURE 7: The effect of hisactophilin (EC-HIS symbolized by spheres; DIC-HIS symbolized by squares) adsorption to the membrane on lateral diffusion of lipid. The fluorescent lipid probe was TR-PE in all cases. The straight arrows show the effect of switching the pH between pH 9 and pH 5 on the lateral lipid mobility for a 1:1 DMPC/DMPG mixture. The undulated arrows show the change of the diffusion coefficient lipid monolayers of different composition after addition of hisactophilin to the subphase. The EC-HIS concentration, c_b, was 93 nM for the 1:1 DMPC/DMPG mixture and 46 nM for the pure DMPC and DMPG monolayers, respectively. For all experiments with DIC-HIS the protein concentration, c_b, was 93 nM.

6. In contrast to the first experiment, the pH value was changed from pH 6 to 9 before an expansion was recorded (curve E_{pH9} in Figure 5). In comparison to the curve of expansion E_{pH6}, the area per lipid molecule is smaller and is in the range of the compression C, which was performed without any protein. Both experiments were performed at a protein concentration of 93 nM EC-HIS.

Lateral Diffusion Measurements. In order to obtain further information on the modification of the membrane structure by hisactophilin binding, we performed lateral diffusion measurements. A simplified photobleaching technique was applied. In this continuous bleaching technique (illustrated in Figure 6 and described in more detail in Appendix A) the fluorescent lipid film is continuously bleached along a stripe. After a sufficient time of irradiation (typically 15 minutes), the fluorescence intensity in the slit region hardly changes any further with time. Then the slit, used as a field stop to achieve a stripelike illumination, is removed, and the distribution of the fluorescence intensity in a direction perpendicular to the long axis of the stripe is recorded by a highly sensitive SIT camera (Hamamatsu). By analysis of the fluorescence intensity profile (cf. images on the right side of Figure 6) in terms of the one-dimensional diffusion equation, the lateral diffusion coefficient D can be obtained. The technique yields only approximate values of D, and it is restricted to small diffusion coefficients ($D < 10$ μm^2/s).

Figure 7 shows the results of two series of experiments. Because of the limitation of the simplified photobleaching technique, the diffusion coefficient for the pure lipid monolayers ($D \approx 15$ μm^2/s) were taken from the literature (Meller, 1985; Merkel & Sackmann, 1993). In one series of experiments, the change of D in a pure DMPG monolayer, a DMPC/DMPG 1:1 mixture, and a pure DMPC monolayer, respectively, after addition of EC-HIS was observed at a pH value of 6. As Figure 7 shows, addition of 46 nM protein into the subphase results in a reduction of D by about a factor of 30 (from $D \sim 15$ μm^2/s to $D \sim 0.4$ μm^2/s). In the case of the DMPC/DMPG mixture, the reduction of mobility (from $D \sim 15$ μm^2/s in the absence of EC-HIS to $D \sim 4$ μm^2/s, in the presence of $c_b = 46$ nM protein) is less drastic. The protein exhibits no detectable effect on an uncharged DMPC monolayer at $c_b = 46$ nM. We also measured the reduction of D by DIC-HIS. Addition of 93 nM of protein in the subphase (pH 6) of a pure DMPG monolayer or a 1:1 mixture with DMPC led in both cases to a reduction of the value of D to about 0.25 μm^2/s.

In the second type of experiment, EC-HIS ($c_b = 93$ nM) was injected into the subphase of a 1:1 DMPC/DMPG mixture and the diffusion coefficient D was measured while the pH was changed from pH 6 to pH 8 and vice versa from pH 8 to pH 5. Clearly, D changes in a reversible way from a reduced value of about 4 μm^2/s at pH 6 to the value characteristic for the pure monolayer at pH 8 and pH 9.

The most pertinent conclusions to be drawn from the experiments in Figure 7 are: 1. The addition of hisactophilin leads to a significant reduction of the diffusion coefficient D, if the lipid monolayer contains DMPG. As demonstrated for the 1:1 mixture of DMPC/DMPG, D is lowered more drastically by DIC-HIS than by EC-HIS. This suggests that natural hisactophilin couples more strongly to partially charged membranes owing to the additional hydrophobic effect. This is verified by more recent neutron reflectivity measurements (Naumann et al., to be published). 2. The reduction of D by at most a factor of 30 (as in the case of pure DMPG) shows that the lipid monolayer remains in a fluid state after protein adsorption. One would expect a reduction to $D \sim 10^{-3}$ μm^2/s—the D value characteristic for lipid in the gel phase (cf. Meller, 1985)—if the lipid layer was solidified. 3. Hisactophilin binds to partially charged membranes in a pH-dependent manner, and the pH at which the binding−unbinding transition occurs agrees with the pK value of histidine.

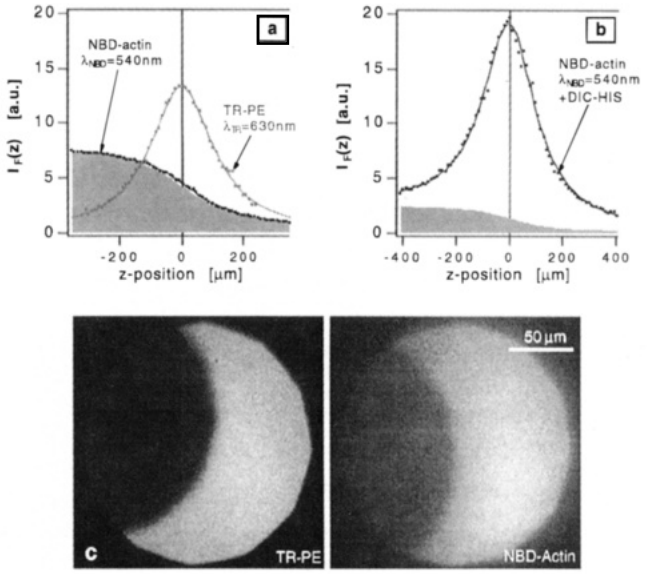

FIGURE 8: Demonstration of hisactophilin-mediated binding of G-actin to membranes. Fluorescence intensity measurements in the z-direction were performed by moving the focus plane of the objective across the air−water interface. Panel (a) shows the z-profiles first of Texas-Red-labeled PE (TR-PE) in DMPC (at 25 mN/m), which forms an insoluble monolayer at the water−air interface, and second of NBD-actin (70 nM) dissolved in the buffer (pH 6). The emission of TR-PE was obtained at 630 nm and that of NBD-actin at 540 nm. Panel (b) shows the z-profile of NBD-actin (70 nM), injected after the addition of 93 nM DIC-HIS in the subphase (pH 6) of a DMPG monolayer (~29 mN/m). The dots are the measured intensities while the drawn curves are the fitted theoretical intensity distributions (cf. Appendix B). The shaded areas in (a) and (b) are calculated intensity curves corresponding to the amounts of NBD-actin dissolved in the buffer. (c) Fluorescence images of DMPG monolayer at ~29 mN/m doped with 0.1 mol% TR-PE. The subphase contains DIC-HIS (c_b = 93 nM) and NBD-actin (70 nM) which were injected subsequently. *Left*: Fluorescence micrograph of TR-PE alone. *Right*: Fluorescence micrograph of NBD-labeled actin, adsorbed to the interface. Part of the monolayer was bleached by irradiation to decompose TR-PE (left) and to bleach NBD-actin (right), respectively. For that purpose the fluorescence images were recorded immediately after a small shift of the microscope in the $x-y$ plane. The former position of the aperture is visualized by the dark bleached area.

Natural Hisactophilin Mediates Binding of Actin to Membranes. The capacity of hisactophilin to mediate the binding of actin to membranes was investigated by intensity distribution measurements, described in detail in Appendix B.

Figure 8a shows typical intensity-versus-position (z) curves for the situation of an insoluble fluorescent film at the water−air interface and a purely soluble dye in the subphase. The former consist of DMPC (at 25 mN/m) doped with 0.1 mol% of TR-PE exhibiting an emission maximum at λ_{TR} = 630 nm, whereas the subphase contained NBD-actin exhibiting maximum emission at λ_{NBD} = 540 nm. The $I_F(z)$-versus-z curves of the two components were recorded separately. The intensity distribution at 630 nm exhibits a Lorentzian distribution showing that TR-PE is localized in the monolayer. The steplike shape of the $I_F(z)$ distribution at 540 nm (dark line in Figure 8a, left side) shows that actin is not accumulating at the surface in the absence of hisactophilin.

To investigate the effect of hisactophilin on the actin coupling to the lipid film, a pure DMPG monolayer was compressed to about 25 mN/m (buffer at pH 6), before DIC-HIS (93 nM) and NBD-actin (70 nM) were subsequently added. After each injection step we waited several hours to ensure equilibration. Figure 8b shows the resulting fluorescence distribution observed by recording the emission at λ_{NBD} = 540 nm. An asymmetrical band is observed which can be decomposed into a Lorentzian line (representing the adsorbed dyes) and a steplike function (shaded curve) resulting from G-actin dissolved in the subphase. The appearance of a sharp band at the interface demonstrates that a high concentration of actin has bound to the lipid monolayer. It can be seen from the micrographs of Figure 8c that the lateral fluorescence distribution of the lipid layer (left) as well as of the adsorbed actin layer (right) is homogeneous.

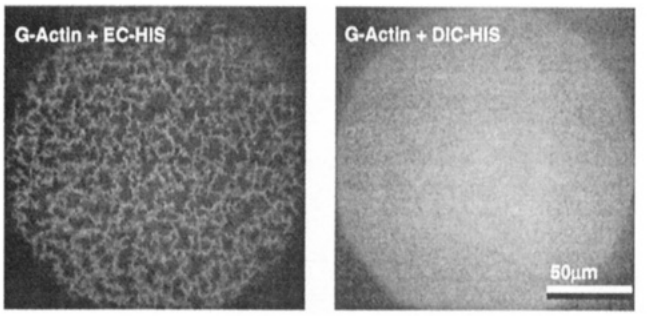

FIGURE 9: Observation of hisactophilin-mediated coupling of fluorescent-labeled G-actin to 1:1 mixed DMPC/DMPG monolayer kept at 29 mN/m and pH 6. Left side: Fluorescence micrographs of NBD-actin in the presence of 93 nM EC-HIS. Right side: Fluorescence micrographs of NBD-actin in the presence of 93 nM DIC-HIS. The actin concentration was 70 nM in both cases.

In additional experiments we compared the effects of EC-HIS and DIC-HIS on the coupling of actin to the monolayer. To that end, a DMPC/DMPG 1:1 mixture was compressed to about 25 mN/m. Then 93 nM DIC-HIS or EC-HIS, respectively, was added to the subphase kept at pH 6. After pressure equilibration (at ~29 mN/m) G-actin was added into the subphase. To ensure a homogeneous distribution in the subphase and to reach binding equilibrium to the surface, fluorescence micrographs were taken several hours after injection of the fluorescent protein. In the case of DIC-HIS one clearly observes a homogeneous coverage at the monolayer with NBD-actin (Figure 9, right micrograph) which provides strong evidence that the natural protein mediates the coupling of G-actin or small oligomers to the monolayer. Further evidence for this conclusion is provided by neutron reflectivity measurements which yield to a thickness of the adsorbed actin layer of 45 Å (Naumann et al., to be published). In the case of EC-HIS, one observes heterogeneous lateral fluorescence distribution, consisting of a network of bright threads separating dark patches (Figure 9, left micrograph). This shows that EC-HIS does not mediate the coupling of actin to membranes in a well-defined way. The bright threads in Figure 9 are attributed to actin bundles formed by coupling to EC-HIS and are randomly oriented by electrostatic adsorption of the hisactophilin−actin aggregates.

DISCUSSION

Estimation of Hisactophilin Binding Energies. The surface excess Γ is defined as the algebraic excess of solute molecules in the surface layer (per unit area) over the moles that would be present in a bulk region containing the same number of moles of solvent as does the section of the surface

region (Adamson, 1990). In fact, this definition holds exactly only for small solutes and for two partially miscible solvents separated by an interface. In equation (1) the insoluble monolayer at the interface is not taken into account. It is assumed that the protein is associated only with the fully hydrated polar region of the lipid layer. Therefore, equation (1) holds in our case only as an approximation. If no multilayer adsorption occurs, the reciprocal value of Γ can be interpreted as the area per adsorbed protein molecule (cf. Figure 4).

A remarkable result of Figure 4 is that Γ depends only very weakly on the molar fraction of DMPG for $x_{PG} > 0.5$ of DMPG. This finding suggests, that each protein interacts with a fixed number of charged lipid molecules which can be roughly estimated as follows: The saturation behavior of the $1/\Gamma$-versus-x_{PG} curve in Figure 4 of hisactophilin indicates saturation at 50% DMPG. From NMR structure determination, one estimates a minimal area of roughly 10 nm^2 per hisactophilin molecules. At $x_{PG} \sim 0.5$, about 50% of the lipid molecules in contact with one protein are charged, corresponding to about 9 DMPG molecules per protein. Note that the area per lipid molecule is 0.6 nm^2 and, therefore, 1.2 nm^2 per DMPG molecule for $x_{PG} \sim 0.5$.

The surface excess Γ is a measure for the difference of the chemical potential of the protein in the bulk solution (μ_b) and at the surface (μ_s). The area concentrations n_s of the protein in the surface layer and in a thin layer (of the same thickness) in the bulk are expected to be related by Nernt's distribution law:

$$\mu_b - \mu_s = k_B T \cdot \ln\left(\frac{n_s}{n_b}\right) \qquad (2)$$

Provided that n_s can be measured, this correlation can be used to determine relative binding energies of the protein as a function of the content of charged lipid in the monolayer.

The molecular diameter of the protein is about 5 nm. In order to estimate the area density (and therefore Γ) at the interface, we consider a $d_s = 5$ nm-thick layer within the solvent, calculate the protein area density in this slice, and by application of the above definition of Γ obtain n_s from the measured value of the surface excess Γ. As an example, we consider the case of a bulk protein concentration of $c_b =$ 22 nM (corresponding to the concentration between the first two injection steps) for the natural DIC-HIS (cf. Figure 3). The area concentration in the 5 nm-thick layer of the bulk solution is $n_b = 6.7 \times 10^{-8}$ molecules/nm^2. In the case of an 80:20 DMPC/DMPG mixture, $\Gamma = 9 \times 10^{-2}$ molecules/nm^2. The excess is then larger than n_b (by a factor of 10^6), and the area concentration at the surface is thus about equal to the measured value of surface excess. Application of equation (2) yields a chemical potential difference of $\Delta\mu \approx 14.5\ k_B T$ for $x_{PG} = 0.2$. The binding energy is only slightly dependent on the molecular fraction of charged lipid for $0.1 < x_{PG} < 0.5$ (cf. Table 1).

Structural Aspects of Hisactophilin−Membrane Interaction. Strong evidence is provided that proteins that couple primarily electrostatically to lipid lamellae can penetrate rather deeply into the semipolar membrane surface, leading to a condensation of the lipid layer at constant membrane area. The observation of an expansive lateral pressure induced by the protein adsorption for both the natural and the fatty acid−depleted protein leads to the conclusion that side chains or flexible loops of the protein penetrate into the lipid layer. The observation, in Figure 2a, that for a given concentration of charged lipid and of hisactophilin, respectively, the same saturation pressure is reached irrespective of the initial pressure π_0 suggests that the protein and the associated lipid form a well-defined entity (or complex) containing a fixed number of charged lipids.

Table 1: Chemical Potential Difference between Protein Bound to the Membrane and in the Bulk of Natural Hisactophilin (DIC-HIS) and Genetic Product (EC-HIS)[a]

$\Delta\mu/x_{PG}$	1	0.5	0.3	0.2
$\Delta\mu[k_BT]$ DIC-HIS	16.1	15.7	15.1	14.6
$\Delta\mu[k_BT]$ EC-HIS	15.8	–	15.0	14.5

[a] The values were evaluated for a subphase concentration c_b of 22 nM.

Most remarkable is, however, that this partial penetration of the protein into the lipid layer occurs up to astonishing high lateral pressures of about 30 mN/m, which is supposed to be about equal to the intrinsic lateral pressure of flaccid (= tension free) vesicles or biomembranes (Sackmann, 1994). Similar behavior was found for talin (Dietrich et al., 1993), another cytosolic protein mediating the binding of actin to membranes where penetration is observed up to at least 25 mN/m. In the case of other proteins such as spectrin adsorbing to charged membranes (Maksymiw et al., 1987) such strong binding is observed only at much lower lateral pressures (~15 mN/m) which are close to the equilibrium spreading pressure of the protein. This shows that hisactophilin (and similarly talin) exhibits very strong surface activity. The partial penetration of the protein into the lipid layer is also supported by numerous studies of the effect of small anions on partially charged monolayers showing a decrease of the lateral pressure with increasing ionic strength (for references see Helm et al., 1986). This is indeed expected for a purely electrostatic effect due to the reduction of the electrostatic repulsive lateral pressure between the charged lipid head groups by charge compensation. In this context, the behavior of the mixture with PIP_2 is most remarkable: In this case, a normal electrostatic effect is found at bulk protein concentrations below 70 nM before the protein starts to penetrate into the lipid layer, and the pressure increases with increasing protein concentration. This finding can be partially attributed to the much higher surface charge or repulsive electrostatic pressure (note that PIP_2 exhibits 5 negative charges per molecule) but may also be attributed to the impediment of the protein penetration into the much bulkier head group region of PIP_2. The actin-binding experiments show that the hisactophilin−membrane coupling is more subtle than revealed by the film balance studies alone which suggest an equally strong membrane coupling of the two membrane species. The natural protein appears to mediate the membrane coupling of G-actin without remarkable formation of oligomers. In contrast, the myristic acid−deficient species appears to induce the formation of short actin filaments or oligomers which then bind to the surface. The difference in the binding mechanisms of the two hisactophilin species is also revealed by the lateral diffusion measurements showing that lipids are more strongly immobilized by DIC-HIS. More direct evidence for a different structural organization of the lipid−protein assemblies of the two hisactophilin species was provided by recent neutron surface scattering experiments which will be

published in an accompanying paper. These show that the native protein penetrates deeply into both the hydrophobic domain and the semipolar head group region of lipid monolayers, whereas the recombinant protein does not penetrate to a remarkable extent. In summary, these experiments demonstrate that the fatty acid chain is essential for the correct orientation of the actin-binding sites.

CONCLUSIONS

In the present work we demonstrated that hisactophilin can mediate the binding of actin to lipid membranes without additional proteins in a pH-dependent way and at high lateral pressures (~25 mN/m) which are of the same size as in biological membranes, free of osmotic stress. The present *in vitro* experiments were performed at ionic strengths (~20 mM) considerably smaller than the physiological values in the cytoplasm (~150 mM) in order to avoid actin polymerization in our studies on the hisactophilin-mediated actin−membrane coupling. The electrostatic contribution to the membrane binding of hisactophilin is thus certainly much smaller under physiological conditions. More important appears to be a low lateral pressure of the membrane bilayers (<30 mN/m). As follows from Figure 5 and as has been shown in additional experiments (not shown), natural hisactophilin bound at low pressures (e.g., 20 mN/m) remains bound up to $\pi = 35$ mN/m before it is squeezed out of the monolayer. The latter value of π is most certainly larger than the pressures characteristic for natural membranes. This hysteresis could have important biological consequences. Hisactophilin could bind during transient reductions of the lateral pressure in the inner leaflet of the plasma membrane generated, for instance, during transient phospholipid turnover by phospholipases. It would, however, remain bound unless removed by other biochemical processes.

ACKNOWLEDGMENT

One of the authors (E.S.) is most grateful to the hospitality of the staff and the colleagues of ITP. We thank D. Riegler and M. Stöckelhuber for help during protein preparation.

APPENDICES

A: Lateral Mobility Measurements. In order to gain quantitative information about the lateral mobility in a two-dimensional layer, it is convenient to perform continuous bleaching experiments as illustrated in Figure 6. Depending on the diffusion coefficient of the fluorescent molecules, different intensity profiles will evolve. High diffusion constants smear out the profile, while in the absence of diffusion a sharp edge arises at the border of the illuminated area. To simplify the geometry for the quantitative analysis of the fluorescence profiles in such bleaching experiments, we illuminated a rectangular area in the lipid layer. With increasing time, a steady-state situation is approximately reached since the bleached molecules are continuously replaced by new fluorescent probes, diffusing into the bleached area. The fluorescence intensity at each position is stationary within the bleached stripe. When such a situation was reached in our experiments, the illumination aperture was removed, and the fluorescence intensity perpendicular to the bleached stripe was recorded by means of a SIT camera. The video images were then analyzed by a commercial image processing system. Figure 6 shows examples for such an intensity profile of a DMPC/DMPG 1:1 lipid monolayer, in the presence of 93 nM (a) EC-HIS or (b) DIC-HIS in the subphase. The pictures were recorded after 15 minutes of illumination and immediately after removal of the aperture, the initial position of which is indicated by the dark vertical lines in Figure 6. The regions in which the intensity profiles are analyzed are marked by a white frame at the right side of the panel. The steady-state condition is determined by the following relationship:

$$\frac{\partial c(x,t)}{\partial t} = 0 = -[I \cdot c(x,t)] + \left[D \cdot \frac{\partial^2 c(x,t)}{\partial x^2}\right] \quad \text{(A1)}$$

where D is the diffusion coefficient, I is the bleach constant and $c(x,t)$ is the concentration of dyes in a direction parallel to the long axis of the bright rectangle. The solution of this simple differential equation, is given by:

$$c_{ss} = \alpha\left\{\exp\left(-\sqrt{\frac{I}{D}}x\right) + \exp\left(\sqrt{\frac{I}{D}}(x - 2x_m)\right)\right\} \quad \text{(A2)}$$

where x_m defines the center of the bleached strip and α is a proportionality factor. Fitting the measured profiles with this analytical function provides a value for I/D. The bleaching constant I is determined in a separate experiment, in which the first-order bleaching kinetic is analyzed. The error of D is about ±50%. It is determined by the uncertainties of I (±20%) and the quotient I/D. One has to keep in mind that there is a systematic deviation, since a steady-state profile is only approximately reached. Numerical simulations demonstrate that for most cases this effect is negligible (Dietrich, unpublished results). In separate experiments it was shown that data obtained by standard FRAP measurements (Axelrod et al., 1976) were very well reproduced by our continuous bleaching technique.

B: Observation of Fluorescent Molecule Distribution at the Liquid−Air Interface. The adsorption of proteins to the surface was detected by recording the fluorescence intensity in the field of view of the objective while moving the objective in a vertical direction in such a way that the focus plane of the objective was scanned perpendicular to the air−water interface. The experiment was performed in the following way: First, the position of the air−water interface was determined by measuring the intensity of the irradiation light reflected from the interface while the objective was moved in the normal direction and by assuming that the reflected intensity is maximal if the focal plane of the objective coincides with the air−water interface. Second, the focal plane of the objective was shifted by 800 μm into the subphase (z-direction). Finally, the fluorescence intensity was measured by moving the objective in steps of ~15 μm into the $+z$-direction by 1600 μm, and the intensity was recorded after each step for 5 s. The fluorescence of different dyes could be separated by a monochromator. The observed fluorescence intensity is a superposition of the emission by molecules adsorbed at the surface and by molecules dissolved in the solution. Separate experiments demonstrated that a single fluorescent layer at the air−water interface results in a Lorentzian-like intensity distribution of half width $\Delta I \approx$ 120 μm (cf. Figure 8a, TR-PE). The maximum agrees very well with that of the reflected intensity defining the position of the interface. A homogeneous subphase can be regarded as an array of many imposed layers extending through the

subphase up to the level of the liquid surface. Therefore, the recorded intensity is obtained by integration over the corresponding Lorentzian-like intensity profiles (cf. Figure 8, shaded curves). If there is an accumulation of fluorescent molecules at the surface, this must be accounted for by an additional Lorentzian line, at the z-position of the surface. By analyzing intensity profiles in this way, it is possible to distinguish between molecules in the subphase and at the surface.

REFERENCES

Adamson, A. W. (1990) in *Physical Chemistry of Surfaces* pp 77−79, John Wiley & Sons, Inc., New York.

Axelrod, D., Koppel, D. E., Schlessinger, J., Elson, E., & Webb, W. W. (1976) *Biophys. J. 16*, 1055−1069.

Detmers, P., Weber, A., Elzinga, M., & Stephens, R. E. (1981) *J. Biol. Chem. 256*, 99−105.

Dietrich, C., Goldmann, W. H., Sackmann, E., & Isenberg, G. (1993) *FEBS Lett. 324(1)*, 37−40.

Goldmann, W. H., Niggli, V., Kaufmann, S., & Isenberg, G. (1992) *Biochemistry 31*, 7665−7671.

Habazettl, J., Gondol, D., Wiltscheck, R., Otlewski, J., Schleicher, M., & Holak, T. A. (1992) *Nature 359*, 855−858.

Hanakam, F., Eckerskorn, C., Lottspeich, F., Müller-Taubenberger, A., Schäfer, W., & Gerisch, G. (1995) *J. Biol. Chem. 270*, 596−602.

Helm, C. A., Lösche, M., & Möhwald, H. (1986) *Colloid Polym. Sci. 264*, 46−55.

Heyn, S. P., & Tillmann, R. W. (1990) *J. Biochem. Biophys. Methods 22*, 145−158.

Isenberg, G. (1991) *J. Muscle Res. Cell Motil. 12*, 136−144.

Kaufmann, S., Käs, J., Goldmann, W. H., Sackmann, E., & Isenberg, G. (1992) *FEBS Lett. 314*, 203−205.

Maksymiw, R., Sui, S. F., Gaub, H., & Sackmann, E. (1987) *Biochemistry 26*, 2983−2990.

Meller, P. (1985) in *Ph.D. Thesis, Technische Universität München.*

Merkel, R., & Sackmann, E. (1994) *J. Phys. Chem. 98*, 4428−4442.

Pardee, J. D., & Spudich, J. A. (1982) *Methods Enzymol. 85*, 164−181.

Sackmann, E. (1994) in *Handbook of Physics of Biological Systems* (Lipowsky, R., Ed.) Vol. 1, Chap. 1, pp 17−18.

Scheel, J., Ziegelbauer, K., Kupke, Th., Humbel, B. M., Noegel, A. A., Gerisch, G., & Schleicher, M. (1989) *J. Biol. Chem. 264*, 2832−2839.

BI950902Q